

Aleksander MAZURKOW<sup>1</sup>  
Adam KALINA<sup>2</sup>

## FRICITION MODELING IN THE START-UP PHASE OF THE SLIDE JOURNAL BEARING

To guarantee a proper operation of a bearing it is necessary that parameters characterizing it in conditions of the start-up phase, a steady state, and run-down phase are known. In the article, plain journal bearing models describing the condition before the start of relative motion ( $\omega_J = 0$ ) were presented. The models were formulated on the grounds of both the Hertz theory and the general theory of elasticity. The bearing operation parameters calculated with the use of the Hertz theory and the solid bush model differ significantly. For the steady state, when  $\omega_J = const$ , operating conditions were determined from equations of the hydrodynamic lubrication theory. Comparative studies indicate that at higher loads, pressures in the journal-bush contact zone may prove to be decisive for proper operation of the bearing, rather than maximum pressures or maximum oil temperatures.

**Keywords:** slide bearings, oil film force, eccentricity ratio, distribution of stresses and deformations, journal bearing, bush bearing

### 1. LIST OF BASIC SYMBOLS

$a$  — ellipse radius vector length [m];  $B$  — bush width [m];  $C_R$  — radial clearance [m];  $C_{URmax}$  — maximum radial clearance with deformation taken into account [m];  $E$  — Young's modulus [N/m<sup>2</sup>];  $E'$  — reduced Young's modulus [N/m<sup>2</sup>];  $F$  — load force (N);  $g_B$  — bush thickness [m];  $h$  — oil film height [m];  $r$  — reference system radial coordinate [m];  $p$  — pressure in oil film [N/m<sup>2</sup>];  $R$  — radius [m];  $R_{B1}$  — bush inner radius [m];  $R_{B2}$  — bush outer radius [m];  $T$  — temperature [°C];  $U_r$  — deformation in radial direction [m];  $U_{rr}$  — relative deformation in radial direction;  $U_\varphi$  — deformation in circumferential direction [m];  $U_{\varphi\varphi}$  — relative deformation in circumferential direction [m];  $x$  — Cartesian system coordinate [m];  $y$  — Cartesian system coordinate [m];  $z$  — Cartesian system coordinate [m];  $2\alpha$  — journal-bush contact angle [rad];  $\eta$  — oil dynamic viscosity [Pa·s];

---

<sup>1</sup>Autor do korespondencji: Aleksander Mazurkow, Wydział Budowy Maszyn i Lotnictwa Politechniki Rzeszowskiej, Aleja Powstańców Warszawy 12, 35-959 Rzeszów, tel.: 178651640, email: al-maz@prz.edu.pl

<sup>2</sup>Adam Kalina, Wydział Budowy Maszyn i Lotnictwa Politechniki Rzeszowskiej, Aleja Powstańców Warszawy 12, 35-959 Rzeszów, tel.: 177432398, email: akalina@prz.edu.pl

$\nu$  — Poisson number;  $\sigma$  — stresses [ $\text{N/m}^2$ ];  $\sigma_{rr}$  — stresses in direction of radial coordinate [ $\text{N/m}^2$ ]. Indexes: B — solid bush, H — Hertz model; J — journal.

## 2. INTRODUCTION

The phenomenon of occurrence of hydrodynamic oil film was first described by N. P. Pietrow [12], B. Towers [16], and O. Reynolds [14]. In subsequent years, the development of the theory of hydrodynamic lubrication was strongly influenced by works of A. Sommerfeld [15], G. Vogelpohl [17], and W. Kaniewski [4]. Currently conducted research pertains mainly to determination of properties of the hydrodynamic oil film with geometrical forms of the oil clearance taken into account [2, 5, 6, 10, 11]. For the state when the journal rotates at a speed of  $\omega_J = \text{const}$ , journal and bush surfaces are separated by an oil layer ( $h_{\min} > h_{\lim}$ ). A proper operation of the bearing is affected by the position of the journal relative to the bush. In the oil film, pressure in the working area reaches the value of  $p = p_{\max}$  and the temperature increases up to  $T = T_{\max}$ .

Studies are also undertaken for the state when the journal is stationary, i.e.  $\omega_J = 0$ . Modeling of operating conditions in such a case is a complex issue. In the course of starting from standstill, when the journal does not rotate, a complex state of stresses occurs in the journal-bush contact area. Journal and bush materials have significantly differing properties. Values of the longitudinal modulus of elasticity for bearing alloys are much smaller than those of steel alloys ( $E_B < E_J$ ), whereas Poisson numbers for bearing bush alloys are higher than those of steels ( $\nu_B > \nu_J$ ). Considerations concerning description of the phenomena occurring in the contact zone are carried out with the use of methods consisting of adopting certain assumptions concerning either distribution of stresses or distribution of deformations.

In the present paper, theoretical models of the state of stresses and deformations of the solid bush and the Hertz model of stresses and deformations are presented. The maximum values of stresses and deformations obtained from the two models are compared.

A characteristic was also developed on which the effect of load on bearing operation parameters is shown in both the starting phase and the steady-state conditions.

## 3. THE HERTZ MODEL OF STRESSES AND DEFORMATIONS

In the Hertz contact model (Figure 1), an ellipsoidal distribution of stresses is assumed in the journal-bush surface contact zone [3, 7, 8, 9, 18]:

$$\sigma_H(x) = \frac{\sigma_{H \max}}{a} \cdot \sqrt{a^2 - x^2}, \text{ gdzie } -a \leq x \leq a \quad (1)$$

For the assumed stress distribution, the maximum values such as the contact path length ( $2a$ ), maximum stresses ( $\sigma_{\max}$ ), and maximum deformations ( $U_{\max}$ ) are determined from the equation of deformations:

$$\frac{E'}{\pi} \cdot \iint_S \frac{\sigma_H(x)}{x} dS = U_H(x) + \rho_z \cdot x^2 \quad (2)$$

where  $E'$  is the reduced Young's modulus:

$$E' = \frac{1 - \nu_1^2}{E_1} + \frac{1 - \nu_2^2}{E_2} \quad (3)$$

and  $\rho_z$  is the reduced radius of curvature:

$$\rho_z = \frac{1}{2} \cdot \frac{R_{B1} - R_J}{R_{B1} \cdot R_J} \quad (4)$$

Adopting the journal-bush contact angle ( $2\alpha$ ) as the quantity of assumed value, other quantities describing operating parameters of the bearing in the starting conditions will be expressed by the following formulas:

$$2a = 2 \cdot R_{B1} \cdot \sin \alpha \quad (5)$$

$$F' = \frac{(R_{B1} - R_J) \cdot R_{B1} \cdot \sin^2 \alpha}{R_J \cdot E'} \quad (6)$$

$$\sigma_{H \max} = F' \cdot \frac{2}{\pi \cdot a} = \frac{F}{B} \cdot \frac{2}{\pi \cdot a} \quad (7)$$

$$U_{H \max} = E' \cdot \frac{\sigma_{H \max} \cdot \pi \cdot a}{2} \quad (8)$$

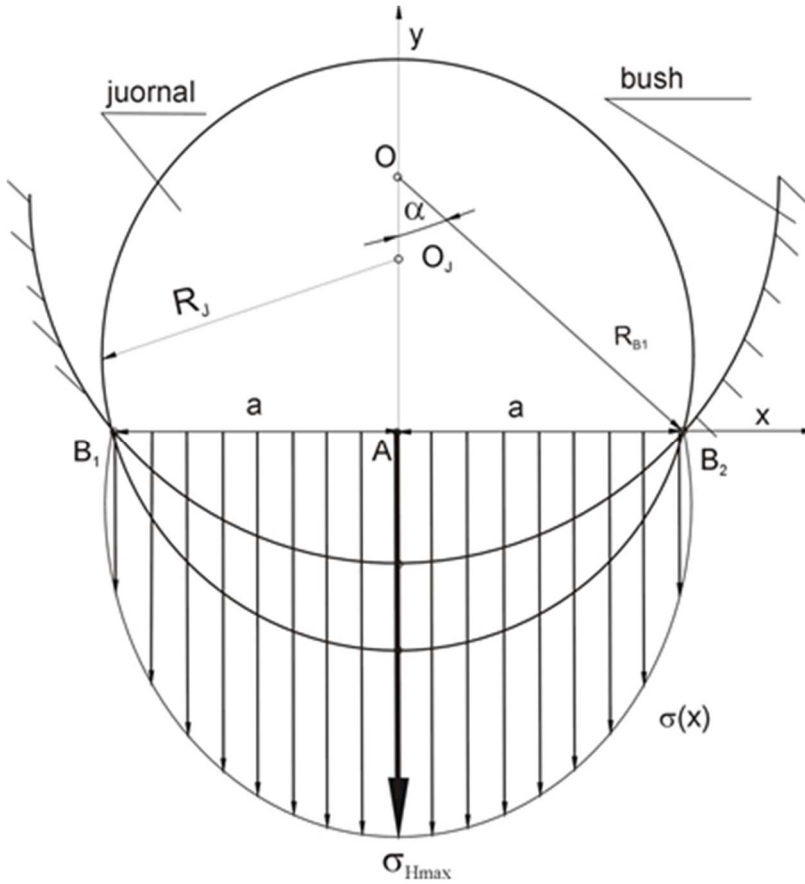


Fig. 1. Geometry and distribution of stresses and deformations for the Hertz model

For such adopted calculation model, the output quantities ( $F$ ,  $\sigma_{Hmax}$ ,  $U_{Hmax}$ ) are functions of the contact surface geometry ( $\rho_v$ ,  $B$ ) and material properties ( $E'$ ).

#### 4. THE MODEL OF STRESSES AND DEFORMATIONS IN THE JOURNAL-SOLID BUSH CONTACT ZONE

Distribution of stresses in the journal-bush contact zone (Fig. 2) can be also determined from equations of the theory of elasticity by adopting the following assumptions [7, 9]:

- journal and bush surfaces are perfectly smooth and circularly cylindrical,
- the bearing journal is non-deformable and only the bush is subject to deformations,
- bush deformation will be considered within the elastic range,

- relative deformations in direction of the variable ( $r$ ) are described (Fig. 2) by the relationship:

$$U_{rr}(\varphi) = \frac{U_r(\varphi)}{R_{B2} - R_{B1}} = \frac{U_r(\varphi)}{g_B} \quad (9)$$

For the adopted assumptions, the relationships sufficient to determine the bush thickness as well as stress and deformation distributions are obtained. The quantities are as follows:

$$\sigma_{rr}(\varphi) = \frac{E}{(1+\nu) \cdot (1-2 \cdot \nu)} \cdot [(1-\nu) \cdot U_{rr}(\varphi) + \nu \cdot U_{\varphi\varphi}(\varphi)] \quad \text{dla } |\varphi| \leq \alpha \quad (10)$$

$$\sigma_{rr}(\varphi) = 0 \quad \text{dla } |\varphi| \geq \alpha$$

$$\sigma_{rr}(\varphi = 0) = \sigma_{rr \max} \quad (11)$$

where:

$$-U_r(\varphi) = -U_{rr}(\varphi) \cdot g_B = \begin{cases} -\frac{C_{ur \max} \cdot \cos \varphi - C_R}{g_B} \text{ dla } |\varphi| \leq \alpha \\ -\frac{C_{ur \max} \cdot \cos \alpha - C_R}{g_B} \text{ dla } |\varphi| \geq \alpha \end{cases} \quad (12)$$

$$C_{ur \max} = \frac{C_R}{\cos \alpha} \cdot \frac{1}{\left(\frac{\nu}{1-\nu}\right)^2 \frac{\operatorname{tg} \alpha - \alpha}{\pi} + 1} \quad (13)$$

$$U_{\varphi\varphi}(\varphi) = \begin{cases} \frac{1}{(1-\nu) \cdot \nu \cdot g_B} \cdot [C_{ur \max} \cdot (\nu^2 \cdot \cos \varphi + \cos \alpha \cdot (1-2\nu)) - C_R \cdot (1-\nu)^2] \text{ dla } |\varphi| \leq \alpha \\ \frac{(1-\nu)}{\nu \cdot g_B} \cdot (C_{ur \max} \cdot \cos \varphi - C_R) \text{ dla } |\varphi| \geq \alpha \end{cases} \quad (14)$$

$$U_{r \max} = C_{ur \max} - C_R \quad (15)$$

$$g_B = R_{B2} - R_{B1} \quad (16)$$

$$C_R = R_{B1} - R_J \quad (17)$$

$$F = \int_{-\alpha-B/2}^{\alpha+B/2} \int \sigma_{rr}(\varphi) d\varphi \quad (18)$$

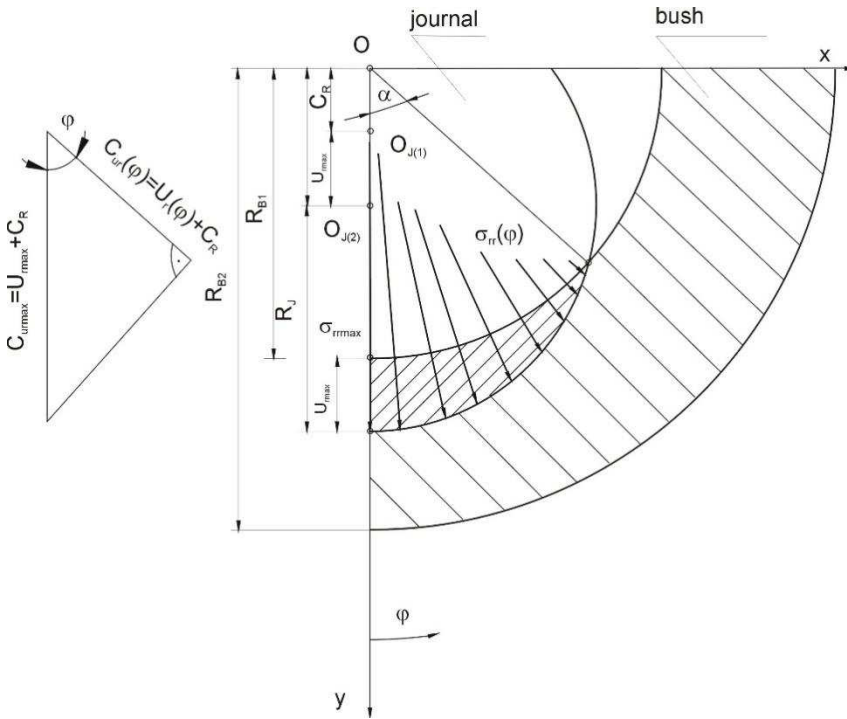


Fig. 2. The state of stresses and deformation in the plain journal bearing bush

As it follows from equations (9–18), radial stresses ( $\sigma_{rr}(\varphi)$ ) are functions of material constants ( $E$ ,  $\nu$ ), and radial and circumferential deformations ( $U_{rr}$ ,  $U_{\varphi\varphi}$ ). The deformations ( $U_{rr}$ ,  $U_{\varphi\varphi}$ ) are functions of radial clearance ( $C_R$ ), the contact angle ( $\alpha$ ), and the Poisson number ( $\nu$ ). Similarly, adopting the model assumption that the bush is non-deformable and only the journal is subject to deformation, it is possible to determine stresses and deformations of the latter. In such a case, the value of the contact path length ( $2a$ ), maximum stresses ( $\sigma_{rrmaxJ}$ ,  $\sigma_{rrmaxB}$ ), and deformations ( $U_{rrmaxJ}$ ,  $U_{rrmaxB}$ ) of journal and bush in the contact area for materials with different properties ( $E$ ,  $\nu$ ) will assume values  $a_J \neq a_B$ ,  $\sigma_{maxJ} \neq \sigma_{maxB}$ , and  $U_{maxJ} \neq U_{maxB}$ .

## 5. BEARING OPERATION IN FLUID FRICTION CONDITIONS

Properties of plain journal bearings (Fig. 3) in fluid friction steady-state conditions ( $\omega J = \text{const}$ ) can be described with the following system of equations [1, 4, 5, 6, 7]:

- oil clearance form:

$$h = 0,5 \cdot D \cdot \psi_{eff} \cdot [1 + \varepsilon \cdot \cos(\varphi - \beta)], \quad \text{gdzie } \psi_{eff} = \frac{C_{eff}}{D} \quad (19)$$

- pressure distribution in the oil clearance:

$$\frac{4}{D^2} \frac{\partial}{\partial \varphi} \left( h^3 \cdot \frac{\partial p}{\partial \varphi} \right) + \frac{\partial}{\partial z} \left( h^3 \cdot \frac{\partial p}{\partial z} \right) = 6 \cdot \eta \cdot \omega_J \cdot \frac{\partial h}{\partial \varphi} \quad (20)$$

- temperature distribution in the oil clearance:

$$\frac{\tilde{v}_x}{R_J} \frac{\partial T}{\partial \varphi} + \tilde{v}_z \cdot \frac{\partial T}{\partial z} = \frac{\eta}{\rho \cdot c_p} \cdot \frac{1}{h} \cdot \int_0^h \left[ \left[ \frac{\partial v_x}{\partial y} \right]^2 + \left[ \frac{\partial v_z}{\partial y} \right]^2 \right] dy \quad (21)$$

- flow velocity components in direction of axes (x) and (z) described by relationships:

$$\begin{aligned} \tilde{v}_x &= \frac{1}{h} \cdot \int_0^h \left[ \frac{1}{2\eta} \frac{\partial p}{\partial x} y(y-h) + \frac{\omega_J \cdot R}{h} y \right] dy, \\ \tilde{v}_z &= \frac{1}{h} \int_0^h \left[ \frac{1}{2\eta} \frac{\partial p}{\partial z} y(y-h) \right] dy, \end{aligned} \quad (22)$$

- oil viscosity as a function of temperature:  $\eta = \eta(T)$

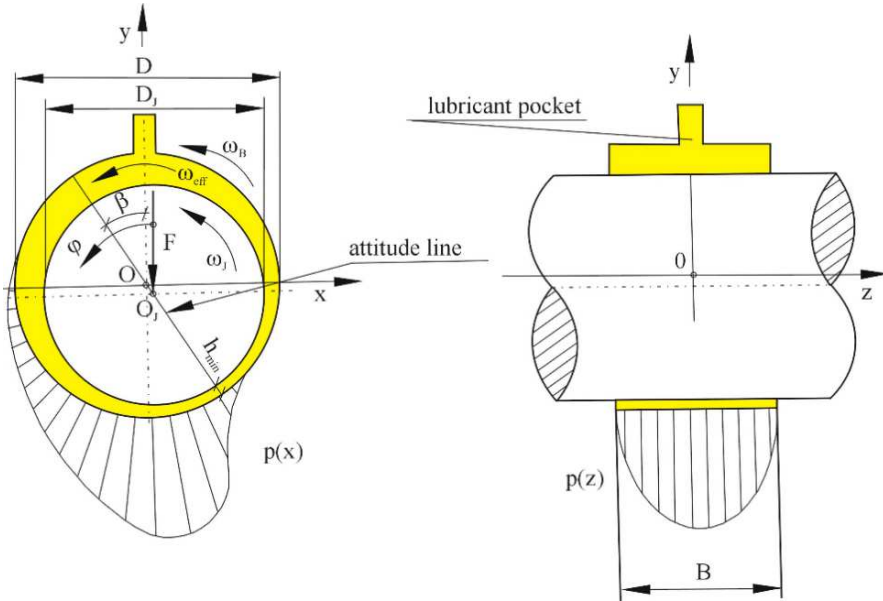


Fig. 3. Geometry and pressure distribution in a plain journal bearing fed with fresh oil from lubrication pocket

By solving the system of equations (19–22) it is possible to determine quantities necessary to work out static and dynamic characteristics of a plain journal bearing [1, 5, 6]. The set of the parameters defining properties of the bearing comprises:

- the relative eccentricity

$$\varepsilon = \frac{e}{C_{Ref}} \quad (23)$$

where  $e = \overline{OO_j}$  — eccentricity,  $C_{Ref} = (R_{B1} - R_j)_{eff}$  — effective radial clearance,  $\beta$  — the attitude line angle,

- the Sommerfeld number:

$$S_0 = \frac{F \cdot \psi_{ef}^2}{B \cdot D_{B1} \cdot \eta_{ef} \cdot \omega_j} \quad (24)$$

- oil film maximum pressure:

$$p_{\max} = p_{\max}(x, y, z), \quad (25)$$



- oil film maximum temperature:

$$T_{\max} = T_{\max}(x, y, z), \quad (26)$$

- oil film minimum height:

$$h_{\min} = h_{\min}(x, y, z), \quad (27)$$

## 6. A COMPUTATIONAL EXAMPLE

The study was carried out for the stationary state with the use of the Hertz model and for cases when either the bearing bush or bearing journal is subject to deformation. Geometry of surfaces is summarized in Table 1, whereas operation of the bearing in fluid friction conditions was analyzed for the journal speed  $\omega_J = 78.54 \text{ s}^{-1}$  ( $n_J = 750 \text{ rpm}$ ), oil VG150.

Table 1. A computational example

Quantity	Type of model assumed for computation	
	Hertz model	Models in which bush or journal deforms
$R_J$ – journal diameter [m]	$209,745 \cdot 10^{-3}$	$209,745 \cdot 10^{-3}$
$R_{B1}$ – bush inner diameter [m]	$210,00 \cdot 10^{-3}$	$210,00 \cdot 10^{-3}$
$R_{B2}$ – bush outer diameter [m]	-	$230,00 \cdot 10^{-3}$
$B$ – bush width [m]	$315,00 \cdot 10^{-3}$	$315,00 \cdot 10^{-3}$
$E_J$ – Young's modulus of journal material [Pa]	$2,1 \cdot 10^{11}$	$2,1 \cdot 10^{11}$
$E_B$ – Young's modulus of bush material [Pa]	$0,38 \cdot 10^{11}$	$0,38 \cdot 10^{11}$
$\nu_J$ – Poisson number of journal material	0,3	0,3
$\nu_B$ – Poisson number of bush material	0,38	0,38
$2\alpha$ – journal-bush contact angle [rad]	0,04- 0,33	0,01- 0,23

The static characteristic was developed in terms of functions  $U_{\max}(F)$ ,  $\sigma_{\max}(F)$ ,  $p_{\max}(F)$ ,  $h_{\min}(F)$ , and  $T_{\max}(F)$ . The functions in the form of plots are presented in Figure 4.

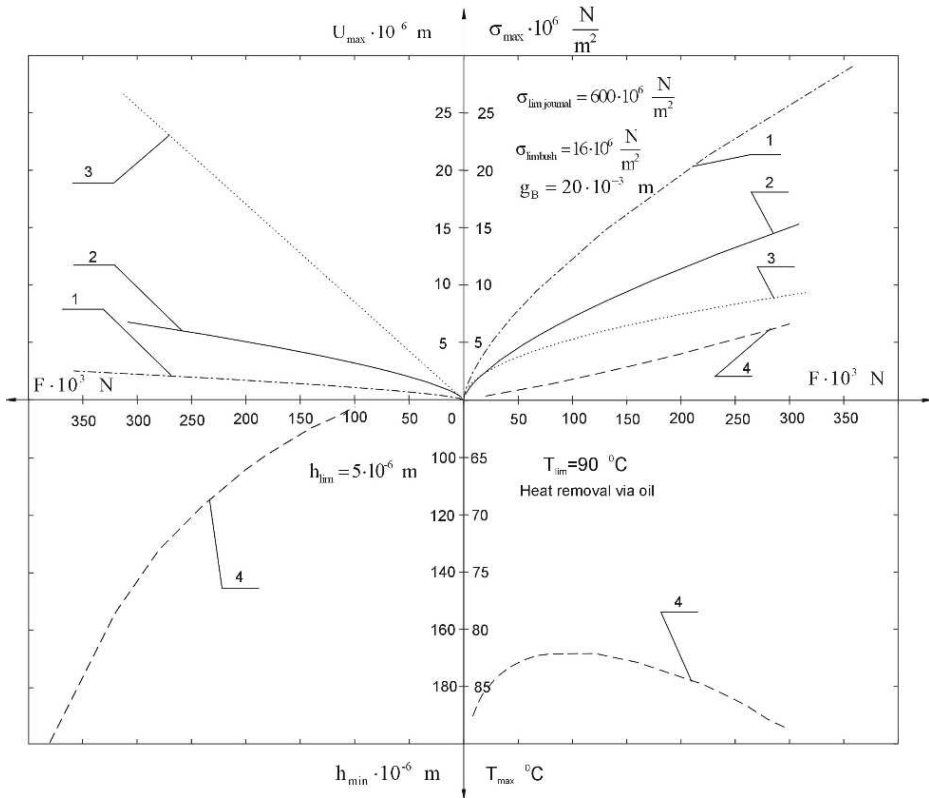


Fig. 4. Dynamic characteristics of the plain journal bearing. The quantities shown in the drawing concern: 1 – journal; 2 – solid bush; 3 – Hertz model; 4 – hydrodynamic oil film

## 7. COMPARATIVE ANALYSIS OF RESEARCH RESULTS

From the analysis of the course of functions presented in Figure 4, the following conclusions can be drawn:

- The oil film minimum height for  $\omega_J = 78.54 [s^{-1}]$  decreases with increasing load value. For the load  $F = 300 [kN]$ , the minimum oil film height is  $h_{min} = 82 [\mu m]$ ,
- the oil film maximum temperature for  $\omega_J = 78.54 [s^{-1}]$  increases with increasing load on the bearing. For the load  $F = 300 [kN]$ , the maximum temperature is  $T_{max} = 89[^\circ C]$ ,
- maximum pressure values in starting conditions ( $\omega_J = 0$ ) and the maximum pressure in oil film ( $\omega_J = 78.54 [s^{-1}]$ ) increase with increasing load. The values calculated for the load  $F = 300 [kN]$  are as follows:

Fluid friction model	Hertz model	Deformable solid bush model	Deformable journal model
$p_{max} = 6,5 \text{ MPa}$	$\sigma_{Hmax} = 9,0 \text{ MPa}$	$\sigma_{Brrmax} = 15 \text{ MPa}$	$\sigma_{Jrrmax} = 25,5 \text{ MPa}$
-	$2a = 133,1 \text{ mm}$	$2a = 95,0 \text{ mm}$	$2a = 55,0 \text{ mm}$

Adopting the Hertz model for calculations results in significantly lower values of maximum stresses compared to the model of non-deformable solid bush and the deformable journal model,

- maximum deformation values are the increasing functions. In case of the Hertz model, the sum of bearing bush and journal deformations is calculated, whereas in models of deformable bush or deformable journal, deformation of either journal or bush is only determined. The calculated maximum deformation values for the load  $F = 300 \text{ [kN]}$  are as follows:

Fluid friction model	Hertz model	Deformable solid bush model	Deformable journal model
$\omega_j = 78,54 \text{ [1/s]}$	$\omega_j = 0$	$\omega_j = 0$	$\omega_j = 0$
$h_{min} = 82,3 \text{ }\mu\text{m}$	$U_{Hmax} = 25,5 \text{ }\mu\text{m}$	$U_{Brrmax} = 6,5 \text{ }\mu\text{m}$	$U_{Jrrmax} = 2,0 \text{ }\mu\text{m}$

The sum of journal and bush deformations calculated from Hertz formulae is larger than the sum of deformations calculated for the solid bush model.

## 8. CONCLUSIONS

To guarantee a proper operation of a bearing it is necessary that parameters characterizing it in conditions of the start-up phase, a steady state, and run-down phase are known. In the article, plain journal bearing models were presented. The models were formulated on the grounds of both the Hertz theory and the theory of hydrodynamic lubrication. These models enable to calculate the operating parameters in the initial start-up phase and in the state of static equilibrium.

For a plain bearing with the inner diameter of the bushing  $D = 0,42 \text{ m}$ , load  $F = 300 \text{ kN}$ , angular velocity  $\omega_j = 78,54 \text{ 1/s}$ , the conditions for maintaining fluid friction were met.

Construction materials for the journal and the bush with significantly different properties were adopted for the tests:

- steel for the journal  $E_j = 2.1 \cdot 10^{11} \text{ Pa}$ ,  $\nu = 0.3$ ,
- bearing alloy for the bush  $E_j = 0.38 \cdot 10^{11} \text{ Pa}$ ,  $\nu = 0.38$ .

For the adopted calculation models of Hertz and the splitted bush, significantly different values of maximum strains and stresses were obtained. These models describe the bearing start-up process in which the permissible pressure and defor-

mation values are decisive for its correct operation. The determination which model more accurately reflects the actual operating conditions of the bearing arrangement during start-up requires additional experimental tests. The results will be presented in the next article after the research.

## REFERENCES

- [1] DIN 31652, Teil 1, 2, 3: Hydrodynamische Radial – Gleitlager im stationärem Betrieb.
- [2] DIN 31653, Teil 1, 2, 3: Hydrodynamische Axial – Gleitlager im stationärem Betrieb.
- [3] Huber M.T.: *Teoria sprężystości*. PWN, Warszawa 1954.
- [4] Kaniewski W.: *Warunki brzegowe diatermicznego filmu smarnego*. Zeszyty naukowe Politechniki Łódzkiej. Zeszyt specjalny, z.14, 1997.
- [5] Kiciński J.: *Dynamika wirników i łożysk ślizgowych*. Instytut Maszyn Przepływowych im. R. Szewalskiego PAN, tom 28. Gdańsk 2005.
- [6] Mazurkow A.: *Właściwości statyczne i dynamiczne, metoda projektowania łożysk ślizgowych z panewką pływającą*. Oficyna Wydawnicza Politechniki Rzeszowskiej, Rzeszów 2009.
- [7] Mazurkow A.: *Łożyskowanie ślizgowe, podstawy teoretyczne, właściwości, uszkodzenia*. Oficyna Wydawnicza Politechniki Rzeszowskiej, Rzeszów 2013. ISBN 978-83-7199-6.
- [8] Mazurkow A.: *Wybrane zagadnienia z teorii smarowania łożysk ślizgowych*. Oficyna Wydawnicza Politechniki Rzeszowskiej, Rzeszów 2015.
- [9] Pałuch M.: *Podstawy teorii sprężystości i plastyczności z przykładami*. Politechnika Krakowska, Kraków 2006.
- [10] Parszewski Z.: *Drgania i dynamika Maszyn*. WNT, Warszawa 1982.
- [11] Pietrow N.P.: *Inżynierijny żurnal, 1883: także Izbranyje Truda pod red. Lejbenzona L.S., ANSSSR, 1948*
- [12] Remizow D.: *Plastmasowyje podszipnikowyje uzly*. Izdatielstwo pricharkowskom gosudarstwiennom uniwersitetie, Charkow, 1982
- [13] Reynolds O.: *On the efficiency of belts or straps as communicators of work*. Engineer No. 27, 1874.
- [14] Sommerfeld A.: *Zur hydrodynamischer Theorie der Schmiermittelreibung*. Z. angew. Math. Phys, 50, 97-155, 1904.
- [15] Towers B. Proc. Instn. Mech. Engrs. 58, 1885.
- [16] Vogelpohl G.: „Betriebssichere Gleitlager Berechnungs- verfahren für Konstruktion und Betrieb” Verlag Berlin / Heidelberg/ New York, 1967.
- [17] Zakrzewski M., Zawadzki J., *Wytrzymałość materiałów*. PWN, Warszawa 1983.

DOI: 10.7862/rf.2021.pfe.3

Received: 15.06.2021

Accepted: 28.11.2021